arXiv:2607.18907v1 [cs.CV] 21 Jul 2026

SynGallery: A Synthetic Gallery of Real Paintings for Instance-Level Artwork Recognition

Patryk Bartkowiak[1], Jakub Markil[1], Bartosz Kotrys[2], Dominik Michels[3], Sören Pirk[4], and Wojtek Palubicki[1]

[1] Adam Mickiewicz University
[2] ArtiCollect
[3] KAUST
[4] Kiel University

Code | Dataset

Abstract. Instance-level artwork recognition requires matching a handheld visitor photograph to a specific work in a large museum collection. This is challenging because painting datasets typically provide clean catalog images for training, while test queries are captured under oblique viewpoints, gallery lighting, reflections, frames, and other scene-level variations. We present SynGallery, a synthetic gallery dataset for artwork retrieval that addresses this gap without collecting additional real photographs. Starting from catalog images of real paintings, we place each artwork into a procedurally generated 3D gallery scene and render it from multiple viewpoints under varied geometric and appearance conditions, while preserving the exact identity of the original work. The resulting dataset contains 24,490 rendered views of 4,898 paintings from the Met benchmark. We show that these synthetic views provide a stronger training signal than the corresponding studio photographs. At the same number of training data points, training only on SynGallery improves art painting recognition from 67.18 to 73.47 GAP^-. When added to the full Met training set, SynGallery improves the published benchmark protocol from 35.97 to 38.48 GAP. Ablation experiments show that the gain comes primarily from geometric viewpoint variation rather than photographic realism: blur, sensor noise, and image compression consistently reduce performance.

Keywords: Computer Vision · Synthetic Data · Art Painting Retrieval

1 Introduction

Museum visitors increasingly use mobile devices to identify artworks in real time. This presents a challenging instance-level recognition problem: matching a single query photo to a specific artwork among hundreds of thousands of candidates. The Met dataset [15] benchmarks this exact setting. It provides training data of studio catalog photographs of museum exhibits, but evaluates on real photos taken by visitors in the galleries, mixed with thousands of distractor images. This

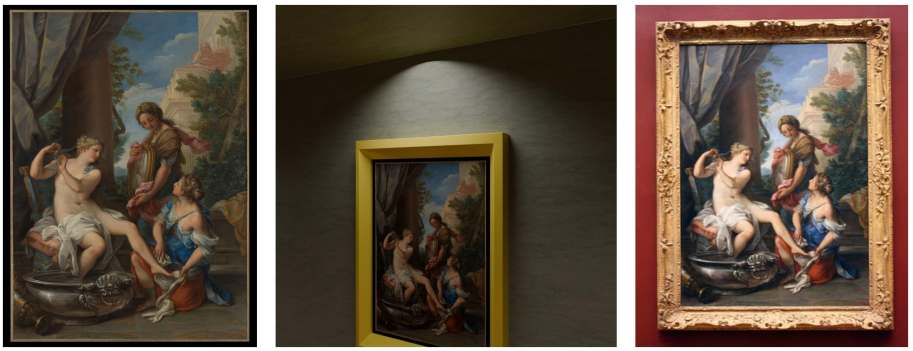


Fig. 1: One painting, three types of photos. The Met benchmark trains on studio catalog photos (left) and is tested with handheld visitor photos (right). SynGallery (center) places the scanned catalog into a synthetic 3D gallery, giving the model training views of each painting on a gallery wall - from angles and lighting that studio photos never show.

task is difficult for two reasons: (1) most artworks have very few catalog photos (over 60% have just one), and (2) the studio training images look nothing like the test ones: clean, frontal studio scans versus handheld shots taken at angles, under gallery lighting, and often through glass.

This difference between studio and visitor photos is the core challenge when training vision models, and collecting many real visitor photos per artwork is impractical at scale. However, since museums already have digitized catalogs of their collections, we procedurally generate a 3D gallery scene for each painting (see Fig. 1) - placed on a wall inside a frame, sometimes behind glass, next to a placard, on varied floors and lighting, rendered from different view points. These renders can be used to train vision models with the scene-level variation that studio scans lack, without collecting a single real-world visitor photo. We introduce this dataset as SynGallery.

The renders are not necessarily meant to have a high perceptual similarity to real photos. Instead, we want to improve performance of vision models on downstream tasks. In fact, embedding analysis using DINOv3 [10] reveals that the SynGallery renders form their own cluster, no closer to the real visitor photos than the studio scans are. This indicates that it is not realism but variation that enhances the training datasets. By changing the scene attributes, the SynGallery training data allows the vision model to learn ignoring the differences between catalog and visitor photos. Furthermore, we demonstrate that this geometric variation drives retrieval performance, whereas forcing the renders to mimic phone camera artifacts actively degrades accuracy.

The SynGallery renders serve as effective training data. At an equivalent image budget, training on the synthetic renders alone beats training on the real studio photos. Added to the full real training set, they outperform the model

released with the Met benchmark, under its exact protocol - with no change to the method and no extra real data.

We make four primary contributions:

1. SynGallery, a dataset of 24,490 gallery renders of 4,898 Met paintings seen from five viewpoints, each saved with its scene details (Sec. 3).
2. A vision model that – at a matched image budget and trained on renders alone – beats training on the real studio photos (closed painting recognition GAP^{-} 73.47 vs. 67.18) (Sec. 5).
3. Adding the renders to the full 397k-image training set improves over the model released with the Met benchmark under its exact protocol (GAP 38.48 vs. 36.1) (Sec. 5).
4. We show through a number of ablation studies that the performance improvement comes from scene variation: covering more viewpoints is the key ingredient, the renders form their own domain rather than imitating visitor photos, and simulating low-level capture artifacts (e.g., blur, sensor noise) actively harms performance (Sec. 5).

2 Related Work

Instance-level recognition and the Met benchmark. Instance-level recognition (ILR) aims to match a query to a specific target within a massive database. Traditionally, ILR is benchmarked on architectural and natural landmarks, using datasets like Google Landmarks v2 [14]. These benchmarks expose the core difficulties of the task: a highly long-tailed class distribution [4] and a high volume of out-of-domain distractor queries. Standard retrieval architectures address this via contrastive learning, typically employing generalized-mean (GeM) pooling with whitening and hard-negative mining [7]. The Met dataset brings these specific ILR challenges into the cultural heritage domain. It requires models to match unconstrained visitor photos to clean studio catalog images — a large domain gap made even harder because most artworks have only one training image.

Artwork and museum recognition. Recognizing artworks under real-world gallery conditions is usually treated as a domain adaptation problem. Open MIC [5] addressed the studio-to-visitor shift by collecting real photos that capture viewpoint changes, gallery lighting, and glass glare. Other large-scale art datasets, such as OmniArt [11], focus on multi-task learning for attributes like style or artist attribution rather than specific instance retrieval. Furthermore, while strong foundation models like Vision Transformers (ViTs) have been evaluated for art tasks such as authentication [8], these approaches typically evaluate 2D style rather than 3D geometry. Instead of collecting real visitor photos, we use 3D renders to generate new viewpoints and lighting.

Synthetic data for retrieval and art. Synthetic training data has been leveraged in cultural heritage contexts, but historically for different tasks. The closest artifact to our pipeline is VirtualGallery [13], which renders a 3D museum environment strictly to train visual camera localization, not to recognize the artworks themselves. When synthetic data is applied directly to art classification, it is almost exclusively 2D-generative: for example, using diffusion models to generate synthetic forgeries to augment authentication datasets [6].

However, 2D generators change the actual content and identity of the artwork. Recent work evaluating the synthetic-to-real domain gap demonstrates that the utility of synthetic training data depends on the non-linear interplay of structural (geometric) consistency and appearance similarity [1]. Because instance-level recognition demands exact identity matching, structural integrity must be preserved. Instead, we use 3D domain randomization [12]: we place the original 2D catalog image into a generated 3D scene. This provides the critical geometric variation (multiple camera poses) and appearance changes (lighting, frames, glass) needed to close the domain gap, while strictly preserving the authentic identity of the cataloged artwork.

3 Dataset Generation Method

SynGallery maps each Met catalog image directly onto a virtual canvas and renders it inside a randomized three-dimensional gallery using Blender 5.1. The catalog image is used as the canvas texture, so the artwork's instance-level identity is preserved exactly, while the room, lighting, frame, and viewpoint around it are sampled anew for every scene. This follows the idea of 3D domain randomization [12], but with an important constraint: because the task is instance-level retrieval, the depicted artwork itself must not change. We therefore keep the catalog image fixed and randomize only the gallery in which it is observed.

3.1 Identity-preserving gallery rendering

An overview of our framework is shown in Fig. 2. Each 3D scene is composed of a rectangular room with a textured canvas placed on one wall, a frame, optional glass, an optional plaque, ceiling lights, and five fixed cameras placed at 30°, 60°, 90°, 120°, and 150° around the painting (examples shown in Fig. 3). The Met catalog image is applied as the canvas texture and the canvas is scaled to the image's aspect ratio, so the depicted content is never cropped, warped, or otherwise altered. The five cameras lie on a horizontal arc at a fixed height and distance from the canvas, all aimed at the painting, so they pan around the painting rather than tilt: 90° is frontal, while 30° and 150° are the extreme oblique views. In rig terms the five poses correspond to rotations of 60°, 30°, 0°, −30°, and −60° about the vertical (global Z) axis. Every painting is rendered from all five cameras, giving $4{,}898 \times 5 = 24{,}490$ RGB images at 512x512 resolution. The renderer, camera distance and field of view, and the default output resolution are listed in Tab. 1. Fig. 4 shows some examples generated using SynGallery.

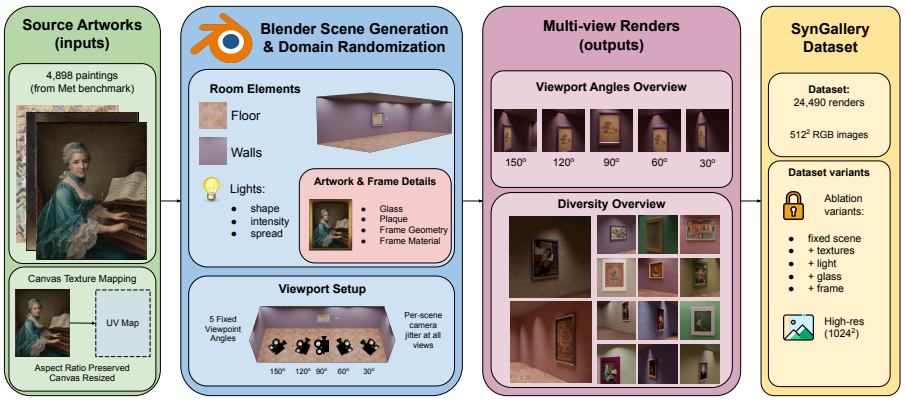


Fig. 2: An overview of our procedural model for gallery artwork paintings used to generate the training dataset SynGallery.

3.2 Scene randomization

For every painting we sample one gallery configuration and render it from the selected cameras. Configuration randomizes the lighting (ceiling-light placement, intensity, and shape), the room appearance (wall, ceiling, and floor materials), the frame (geometry and material), the plaque (visibility, color, and placement), the presence of glass, and a small camera jitter. Tab. 1 specifies, for each factor, the distribution it is drawn from and its range or set of values. The camera jitter is drawn from a uniform distribution, sampled once per view. Ceiling lights are positioned by Poisson-disk sampling, which enforces a minimum spacing. Glass is included as an independent Bernoulli event with probability $p = 0.25$, and the frame geometry is drawn uniformly from a library of 27 shapes. The source painting is loaded from the Met catalog and rescaled to preserve its aspect ratio.

4 Evaluation Protocol

4.1 Model Architecture and Training

To ensure a direct and fair comparison, we reproduce the architecture of the best single model from the original Met benchmark. We use a ResNet-18 backbone [3] pre-trained using Semi-Weakly Supervised Learning (SWSL) [9]. The model is trained via a contrastive loss [2] with generalized-mean (GeM) pooling and a whitening fully-connected layer. During training with synthetic data, positive pairs are formed by mining the closest samples across both the real and synthetic domains. At inference time, we extract multi-scale descriptors to compute the cosine similarity scores.

Table 1: Generation parameters. Artwork identity is the only factor that is never randomized; the remaining factors change the viewing conditions under which the same painting is observed.

Factor	Distribution	Range / values
Viewpoint	fixed	five angles $30°, 60°, 90°, 120°, 150°$ about the vertical axis; optional choice of any subset
Camera location / FOV	fixed	location, field of view
Camera jitter	uniform	translation along $Z \in [-1; 1]$; translation along $Y \in [-0.5; 0.5]$; rotation about $Z \in [-5°; 5°]$; separate values for each camera
Light placement	Poisson-disk	min. spacing, max. density
Light intensity	uniform	single value shared by all lights $\in [0.25; 0.8]$
Light shape	discrete, optional fixed; uniform	{square, disk}, optional choice of base shape; rotation, width, depth
Wall / ceiling color	uniform	separate values for each RGB channel $\in [0; 1]$
Floor material	discrete uniform	over 5 materials
Frame geometry	discrete uniform	over 27 frame shapes
Frame material	uniform	separate values for each RGB channel, roughness and metallic $\in [0; 1]$
Plaque visibility	Bernoulli	present with probability $p = 0.5$
Plaque color	uniform	separate values for each RGB channel $\in [0; 1]$
Plaque placement	discrete	offset relative to painting along $\pm$ X, random choice from a set of three values along Z
Glass presence	Bernoulli	present with probability $p = 0.25$
Renderer / samples	fixed	sample count; engine (e.g. Cycles), render modes (e.g. RGB, semantic mask)
Render resolution	fixed	default 512^2; high-resolution variant 1024^2
Artwork identity	deterministic	Met image as canvas texture, aspect ratio preserved

4.2 Metrics

We evaluate our models using the open-set retrieval protocol of the Met benchmark. Performance is measured using average classification accuracy (ACC) and Global Average Precision (GAP), two standard metrics for instance-level recognition. Following the benchmark, classification is performed using a k-nearest-neighbor (kNN) classifier operating on image embeddings. Given a query image q and a database image x, their similarity is measured using the cosine score $v(x)^\top v(q)$. The confidence assigned to class c is

$$s_c(q) = \max_{x \in NN_k(q)} v(x)^\top v(q), \tag{1}$$

where $NN_k(q)$ denotes the set of the k nearest neighbors of q in embedding space. The resulting class confidences are normalized using a temperature-scaled softmax (with temperature coefficient τ).

Retrieval quality is measured by ranking all queries according to their normalized prediction confidence. GAP is computed as $\text{GAP} = \frac{1}{M} \sum_{i=1}^{T} p(i) r(i)$,

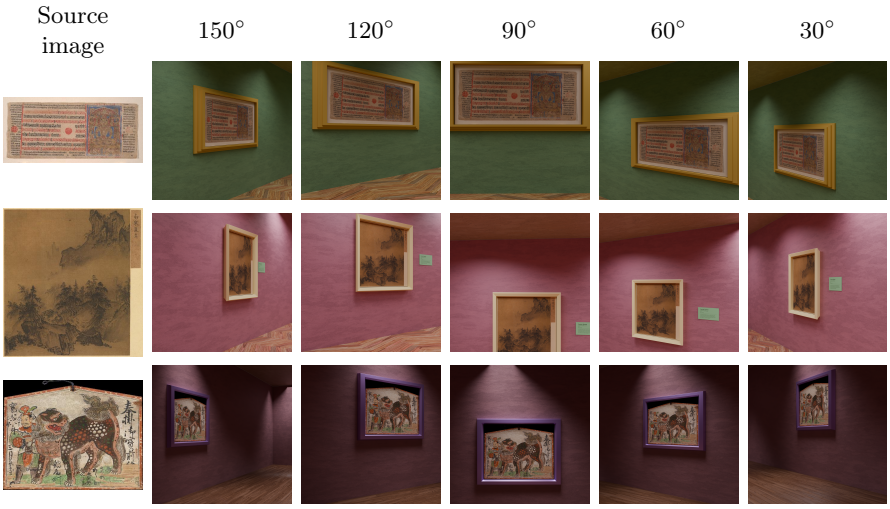


Fig. 3: Met source images (left) and the SynGallery renders generated from them. The catalog image is used directly as the canvas texture, so each artwork's identity is preserved exactly while the surrounding gallery scene is randomized.

where $p(i)$ is the precision at rank i, $r(i)$ indicates whether the prediction at position i is correct, M is the number of target Met queries, and T is the total number of evaluated queries. We report two variants of this metric. GAP$^-$ is evaluated only on target artwork queries and therefore measures closed-world painting recognition. GAP additionally includes out-of-distribution distractors and corresponds to the full open-set retrieval setting of the benchmark. Here, a distractor is a query image that does not depict any of the target Met artworks represented in the retrieval database. Since distractor queries are always counted as incorrect predictions, high GAP requires both accurate artwork recognition and reliable confidence calibration.

The retrieval hyper-parameters k and τ are selected using the validation protocol of the Met dataset. For the ablation experiments, we use 2-fold cross-validation on the painting queries. An audit of this tuning procedure is provided in Appendix A.

5 Results

5.1 Performance on the Met Benchmark

We first evaluate whether SynGallery renders improve retrieval under the full Met benchmark protocol. As shown in Tab. 2, adding SynGallery to the same training recipe increases full-benchmark GAP from 35.97 to 38.48. This provides a direct comparison in which the only change is the addition of synthetic gallery views, yielding a +2.51 GAP improvement. The result also exceeds the best



Fig. 4: A sample of SynGallery images illustrating the variance of procedural data generation.

published single model under the same protocol (GAP 36.1), without changing the retrieval architecture or adding external real-world pre-training data. Fine-tuning the epoch-10 baseline on the synthetic renders alone gives the highest GAP of 38.99. The corresponding non-distractor metrics also improve over the real-only reproduction (GAP^{-} 55.15, ACC 57.23). This indicates that the renders provide useful invariances to gallery-specific variation, such as viewpoint and illumination, while preserving the instance identity needed for retrieval.

5.2 Real vs. Synthetic Mixing and Scaling

To isolate the contribution of the synthetic images relative to the catalog photographs from which they are derived, we evaluate real-to-synthetic training mixtures at a fixed budget of 12,403 images. This budget corresponds exactly to the complete set of real studio photographs available in the full 397k database for the 4,898 painting classes used to generate SynGallery. As shown in Tab. 3

Table 2: Full Met benchmark: 1,003 Met queries plus 18,316 distractors against the 397k-image database. Adding SynGallery to the same training set beats the best published single model under its exact setup.

model (training data)	GAP	GAP⁻	ACC
best published single model	36.1	52.4	55.0
our reproduction (397k real)	35.97	52.14	54.64
from scratch, 397k real + SynGallery	38.48	55.04	57.63
fine-tuned, + SynGallery only	**38.99**	**55.15**	**57.23**
fine-tuned, + SynGallery + real	38.66	53.73	55.53

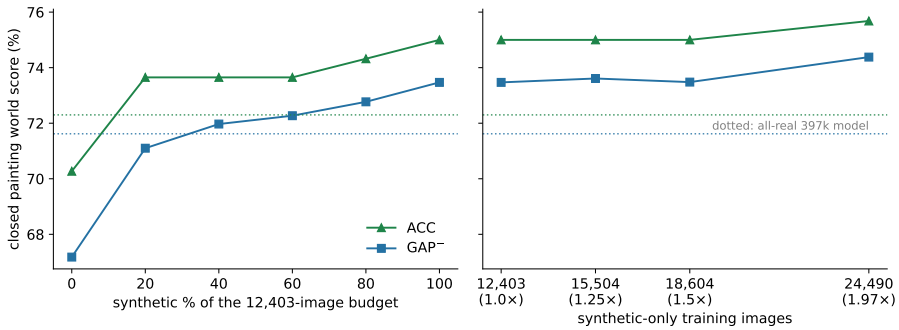


Fig. 5: Performance comparison on the full Met benchmark. Evaluated using 1,003 Met queries and 18,316 distractors against the complete 397k-image database. Adding the SynGallery renders to the baseline training set significantly improves upon the best published single model trained under the exact same protocol (GAP 38.48 vs. 36.1). This demonstrates that synthetic geometric variation alone drives the performance gain, without requiring architectural changes or external real-world pre-training data.

and Fig. 5, replacing real studio photographs with synthetic renders consistently improves performance. The all-synthetic mix achieves a closed-world GAP$^-$ of 73.47, compared to 67.18 for the all-real baseline, showing that multi-view gallery renders provide a stronger training signal than the original studio views at the same image budget. Increasing the amount of synthetic-only training data beyond the fixed budget, up to the full set of 24,490 renders, gives further gains. At this scale, the synthetic-only model reaches GAP$^-$ 53.78 and ACC 56.63 on the full benchmark. It therefore exceeds the 397k real-image baseline on both non-distractor metrics, using approximately 16× fewer training images. Its open-set GAP remains lower (34.38 vs. 35.97), which is expected since the synthetic-only model does not include distractor-class training data such as photographs of busts or statues.

Table 3: Real-to-synthetic data mixing and scaling. Evaluated across both the closed painting world and the full Met benchmark. At a strictly matched 12,403-image budget, the all-synthetic mix uniformly outperforms the all-real baseline. Scaling the synthetic-only data to 24,490 renders surpasses the 397k all-real model on both GAP^{-} and ACC, though open-set GAP trails slightly due to the lack of distractor-class training data.

	closed painting world		full benchmark		
training data	GAP^{-}	ACC	GAP	GAP^{-}	ACC
100:0 — all real	67.18	70.27	28.83	49.08	52.14
80:20	71.10	73.65	30.33	50.41	53.44
60:40	71.97	73.65	31.23	50.84	53.54
40:60	72.27	73.65	31.26	51.12	53.64
20:80	72.77	74.32	32.29	51.85	54.34
0:100 — all synthetic	73.47	75.00	32.75	52.37	54.94
synth-only, 15,504 (1.25×)	73.61	75.00	33.26	52.78	55.23
synth-only, 18,604 (1.5×)	73.48	75.00	33.62	53.18	55.73
synth-only, all 24,490 (1.97×)	**74.38**	**75.68**	34.38	**53.78**	**56.63**
all-real reference (397k)	71.62	72.30	**35.97**	52.14	54.64

5.3 Embedding-Space Coverage Across Domains

To qualitatively examine the relationship between the catalog photographs, synthetic renders, and real painting queries, we extract DINOv3 ViT-L embeddings and project them into two dimensions using t-SNE. As shown in Fig. 6, the three domains exhibit distinct but partially overlapping distributions.

The catalog photographs form relatively compact local clusters, many of which lie near the boundary of the projection. Real painting queries frequently occur within or close to these catalog-image neighborhoods, indicating that the pretrained representation retains correspondence between controlled catalog photographs and real photographs of paintings. In contrast, the synthetic renders occupy a broader and more continuous region of the embedding space. They extend beyond the compact catalog clusters and populate many of the intermediate regions between them.

This distribution is consistent with the intended role of SynGallery. The renders preserve artwork identity while expanding the range of appearances induced by viewpoint, framing, illumination, and gallery context. Rather than reproducing only the compact distribution of the source catalog images, the synthetic data provide broader representation-space coverage, including regions close to many real painting queries. This offers a qualitative explanation for the performance improvements observed when synthetic renders supplement or replace catalog photographs during training.

5.4 Dataset Ablation: The Mechanisms of Transfer

To better understand where the improvement of our synthetically generated dataset lies, we conducted several ablation experiments (see Fig. 7) with our procedural model to identify which aspects contribute to recognition performance.

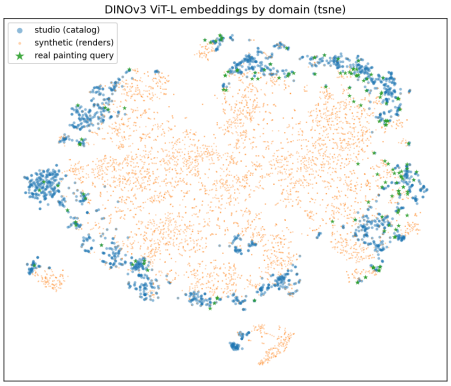


Fig. 6: Embedding-space distribution across image domains. Two-dimensional t-SNE projection of DINOv3 ViT-L embeddings for studio catalog photographs, synthetic SynGallery renders, and real painting queries. Catalog photographs form compact local clusters, whereas the synthetic renders span a broader and more continuous region of the projected representation space. Real painting queries frequently occur near catalog-image clusters and within regions also covered by the synthetic renders.

The results in Tab. 4 indicate that viewpoint variation has the strongest effect among the tested factors. When the five camera views are reduced to a single frontal view, performance drops to GAP^- 68.55, close to the all-real baseline. In contrast, scene-level randomizations, including textures, lighting, and frame variation, have a more mixed effect and provide only modest gains. Rendering at a higher resolution (1024^2) also produces only a small improvement. These results suggest that, for this task, exposing the model to multiple views of the same painting is more important than increasing scene detail or photorealism.

5.5 The Failure of Pixel-Level Augmentation

A natural alternative is to make the renders more similar to mobile photographs by adding low-level capture artifacts. We test this by injecting JPEG compression, sensor noise, resolution loss, and motion blur during training. The tested degradations consistently reduce retrieval performance. JPEG compression produces a relatively small decrease of 0.2 GAP^-, while sensor noise combined with resolution loss reduces performance by 1.7 GAP^-, and motion blur causes a larger drop of 2.9 GAP^-. Applying all three degradation families together yields the largest decrease, reducing GAP^- by 3.8. These results suggest that, in this setting, the domain gap is not best addressed by corrupting the image signal. A likely explanation is that instance-level painting recognition depends on fine visual evidence, including brushwork, texture, and small compositional details. The benefit of SynGallery therefore comes from scene-level variation, especially geometry and illumination, rather than from imitating the low-level statistics of handheld camera images.

Table 4: Dataset ablation in the closed painting world. Models are trained exclusively on 24,490 synthetic renders, varying only the procedural generation parameters. Evaluated using 148 real painting queries against the 12,403-image database, with k/τ chosen via 2-fold cross-validation. The ablation demonstrates that geometric variation (multiple viewpoints) is a primary driver of performance, whereas the effects of scene-level randomizations (such as textures, lighting, and frames) exhibit a more nuanced impact on instance-level retrieval.

	closed painting world	
training renders	GAP^-	ACC
fixed scene (no randomization)	73.78	75.00
+ textures	73.94	75.00
+ light	74.42	75.68
+ glass (p=0.25)	75.32	**76.35**
+ frame	72.61	73.65
+ camera jitter (default SynGallery)	74.38	75.68
default, frame variety frozen	73.91	75.00
default at 1024^2	**75.41**	**76.35**
default, 3 viewpoints (14,694)	74.31	75.68
default, frontal only (4,898)	68.55	70.27
all-real reference (12,403 photos)	67.18	70.27

6 Conclusion

We have presented SynGallery, a synthetic dataset and generation pipeline for instance-level artwork recognition under gallery conditions. The central idea is to preserve the identity of each cataloged painting while changing the scene in which it is observed: camera pose, wall placement, frame, lighting, glass, and surrounding gallery context. This provides training views that are absent from studio catalog photographs, but are characteristic of real visitor queries.

Our experiments show that this synthetic geometric variation is a useful training signal for large-scale artwork retrieval. At a matched image budget, training on SynGallery alone outperforms training on the corresponding real studio photographs. When added to the full Met training set, SynGallery improves the published Met benchmark protocol without changing the retrieval method or introducing additional real visitor photographs. The ablations further indicate that the gain is driven primarily by viewpoint variation rather than photorealistic imitation: the rendered images remain a distinct visual domain in the embedding space, while simulated low-level capture artifacts such as blur, noise, and compression reduce performance.

The current dataset is limited to RGB renderings of paintings and does not yet exploit the full information available from the procedural scene, such as depth, masks, physical camera parameters, or explicit visibility annotations. In future work, we plan to extend the generation process to additional object types, richer gallery configurations, stronger occlusions and reflections, and multimodal annotations.

Additionally, generating synthetic views of distractor classes (such as statues, furniture, and artifacts) would likely close the remaining performance gap in open-set retrieval tasks.

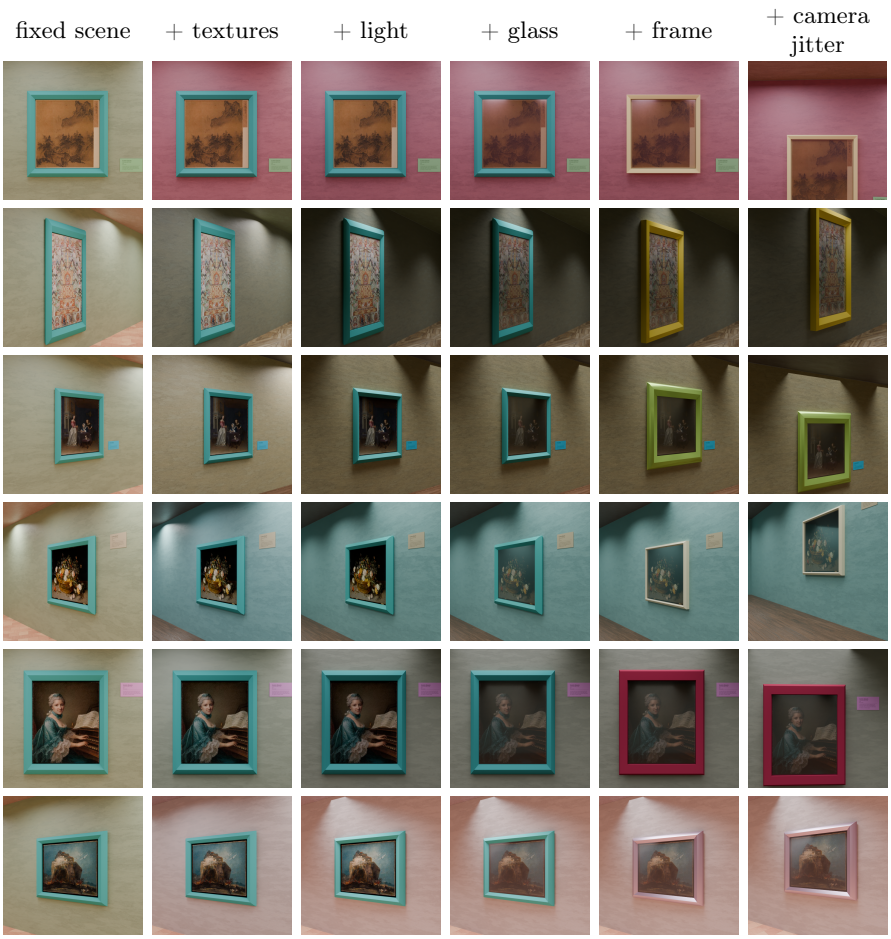


Fig. 7: Comparison of the data from the following steps of ablation study. Each row shows the same scene with different modifications. The rightmost column shows data generated with default the configuration of SynGallery.

References

1. Bartkowiak, P., Kotrys, B., Michels, D., Pirk, S., Palubicki, W.: Sadge: Structure and appearance domain gap estimation of synthetic and real data (2026), https://arxiv.org/abs/2605.22467 4
2. Chen, T., Kornblith, S., Norouzi, M., Hinton, G.: A simple framework for contrastive learning of visual representations. In: Proceedings of the 37th International Conference on Machine Learning. ICML'20, JMLR.org (2020) 5
3. He, K., Zhang, X., Ren, S., Sun, J.: Deep residual learning for image recognition. 2016 IEEE Conference on Computer Vision and Pattern Recognition (CVPR) pp. 770–778 (2015), https://api.semanticscholar.org/CorpusID:206594692 5
4. Kang, B., Xie, S., Rohrbach, M., Yan, Z., Gordo, A., Feng, J., Kalantidis, Y.: Decoupling representation and classifier for long-tailed recognition (2020), https://arxiv.org/abs/1910.09217 3
5. Koniusz, P., Tas, Y., Zhang, H., Harandi, M., Porikli, F., Zhang, R.: Museum exhibit identification challenge for the supervised domain adaptation and beyond. In: Computer Vision – ECCV 2018: 15th European Conference, Munich, Germany, September 8-14, 2018, Proceedings, Part XVI. p. 815–833. Springer-Verlag, Berlin, Heidelberg (2018). https://doi.org/10.1007/978-3-030-01270-0_48, https://doi.org/10.1007/978-3-030-01270-0_48 3
6. Ostmeyer, J., Schaerf, L., Buividovich, P., Charles, T., Postma, E., Popovici, C.: Synthetic images aid the recognition of human-made art forgeries. PLOS ONE **19**(2), 1–15 (02 2024). https://doi.org/10.1371/journal.pone.0295967, https://doi.org/10.1371/journal.pone.0295967 4
7. Radenovic, F., Tolias, G., Chum, O.: Fine-tuning cnn image retrieval with no human annotation. IEEE Transactions on Pattern Analysis and Machine Intelligence **41**, 1655–1668 (2017), https://api.semanticscholar.org/CorpusID:6426453 3
8. Schaerf, L., Postma, E., Popovici, C.: Art authentication with vision transformers. Neural Computing and Applications **36**(20), 11849–11858 (2024). https://doi.org/10.1007/s00521-023-08864-8, https://doi.org/10.1007/s00521-023-08864-8 3
9. Shen, Y., Elhamifar, E.: Semi-weakly-supervised learning of complex actions from instructional task videos. In: Proceedings of the IEEE/CVF Conference on Computer Vision and Pattern Recognition (CVPR). pp. 3344–3354 (June 2022) 5
10. Siméoni, O., Vo, H.V., Seitzer, M., Baldassarre, F., Oquab, M., Jose, C., Khalidov, V., Szafraniec, M., Yi, S., Ramamonjisoa, M., Massa, F., Haziza, D., Wehrstedt, L., Wang, J., Darcet, T., Moutakanni, T., Sentana, L., Roberts, C., Vedaldi, A., Tolan, J., Brandt, J., Couprie, C., Mairal, J., Jégou, H., Labatut, P., Bojanowski, P.: Dinov3 (2025), https://arxiv.org/abs/2508.10104 2
11. Strezoski, G., Worring, M.: Omniart: A large-scale artistic benchmark. ACM Trans. Multimedia Comput. Commun. Appl. **14**(4) (Oct 2018). https://doi.org/10.1145/3273022, https://doi.org/10.1145/3273022 3
12. Tobin, J., Fong, R., Ray, A., Schneider, J., Zaremba, W., Abbeel, P.: Domain randomization for transferring deep neural networks from simulation to the real world. In: 2017 IEEE/RSJ International Conference on Intelligent Robots and Systems (IROS). p. 23–30. IEEE Press (2017). https://doi.org/10.1109/IROS.2017.8202133, https://doi.org/10.1109/IROS.2017.8202133 4
13. Weinzaepfel, P., Csurka, G., Cabon, Y., Humenberger, M.: Visual localization by learning objects-of-interest dense match regression. In: 2019 IEEE/CVF Conference on Computer Vision and Pattern Recognition (CVPR). pp. 5627–5636 (2019). https://doi.org/10.1109/CVPR.2019.00578 4

14. Weyand, T., Araujo, A., Cao, B., Sim, J.: Google Landmarks Dataset v2 - A Large-Scale Benchmark for Instance-Level Recognition and Retrieval. In: Proc. CVPR (2020) 3
15. Ypsilantis, N.A., Garcia, N., Han, G., Ibrahimi, S., van Noord, N., Tolias, G.: The met dataset: Instance-level recognition for artworks. In: Vanschoren, J., Yeung, S. (eds.) Proceedings of the Neural Information Processing Systems Track on Datasets and Benchmarks. vol. 1. Curran (2021), https://datasets-benchmarks-proceedings.neurips.cc/paper_files/paper/2021/file/5f93f983524def3dca464469d2cf9f3e-Paper-round2.pdf 1

A Honest-Tuning Audit

In our closed-world painting recognition and dataset ablation experiments, we determine the retrieval hyper-parameters k and τ using 2-fold cross-validation directly on the 148 test queries. Because the test set is relatively small, a potential concern is that this cross-validation strategy might overfit the hyper-parameters to the query set, artificially inflating the reported GAP^{-} performance.

To verify the integrity of our evaluation, we conduct an "honest-tuning audit." In Table 5, we compare our reported 2-fold cross-validated scores against a leaky "oracle." The oracle score represents the theoretical upper bound achievable by hyper-parameter tuning for this specific dataset. It is obtained by running a grid search over the entire 148-query test set and reporting the absolute maximum score.

The difference between our cross-validated scores and the oracle ceiling is negligible across all data mixes, never exceeding a difference of 0.33 GAP^{-}. In several instances, the 2-fold score marginally underestimates the oracle, which is expected from a strict data split. This confirms that our tuning strategy does not introduce data leakage, and the performance gains demonstrated by the synthetic renders are driven by the data itself, not by k/τ optimization.

Table 5: Honest-tuning audit (closed world). Reported 2-fold cross-validated score vs. the leaky "oracle" (tune = report on all 148 queries). Every gap is ≤ 0.33, so the k/τ choice is not what produces the gains.

mix	reported (2-fold)	oracle	diff
80:20	71.10	71.37	+0.27
60:40	71.97	71.95	−0.02
40:60	72.27	72.21	−0.06
20:80	72.77	72.91	+0.14
0:100	73.47	73.68	+0.21
synth125	73.61	73.70	+0.09
synth150	73.48	73.81	+0.33
synthall	74.38	74.51	+0.13